Research Article

Magnetic Resonance in Chemistry

Received: 16 April 2013 Revised: 20 May 2013 Accepted: 3 June 2013 Published online in Wiley Online Library: 8 July 2013

(wileyonlinelibrary.com) DOI 10.1002/mrc.3983

The structures of two aldazines: [1,1′-(1*E*,1′*E*)-hydrazine-1,2-diylidenebis(methan-1-yl-1-ylidene)dinaphthalen-2-ol] (Lumogen) and 2,2′-(1*E*,1′*E*)-hydrazine-1,2-diylidenebis(methan-1-yl-1-ylidene)diphenol (salicylaldazine) in the solid state and in solution

Artur M. S. Silva,[a] Vera L. M. Silva,[a] Rosa M. Claramunt,[b] Dolores Santa María,[b]* Marta B. Ferraro,[c] Felipe Reviriego,[d] Ibon Alkorta,[d] and José Elguero[d]**

A combination of NMR spectroscopy and theoretical methods Density functional theory including dispersion corrections (DFT-D) was used to study the structures of Lumogen and salicylaldazine. In the solid state, Lumogen exists as the dihydroxy tautomer 1a (an azine, C=N–N=C) as was already known from an X-ray determination. In a deuterated dimethyl sulfoxide solution, another tautomer is observed besides 1a; its structure corresponds to the hydroxy-oxo tautomer 1b (a hydrazone, C=N–NH–Csp^2). In what concerns salicylaldazine, we have observed only the dihydroxy tautomer 2a. Copyright © 2013 John Wiley & Sons, Ltd.

Keywords: Lumogen; salicylaldazine; NMR; CPMAS; DFT-D calculations; temperature effects

Introduction

We have been interested in the structure and configuration of azines of aldehydes (aldazines) and ketones (ketazines), i.e. compounds presenting the >C=N–N=C< motive.[1–10] After, we reported the mesogenic properties of some mixtures of azines.[11–14] Recently, we have devoted some papers to study theoretically their properties, particularly the mechanism of isomerization about the C=N bonds.[15–18] Convinced that azines deserve more attention, we decided to study the cases of Lumogen (**1**) and salicylaldazine (**2**). These two compounds have closely related structures (Fig. 1).

Lumogen [often written as Liumogen, Lumogen Yellow S, Liumogen LT or Liumogen bright yellow (CAS 2387-03-3)] (1) is a commercial pigment material with fluorescent properties that facilitate its use for wavelength-converting optical coatings. A common application is in UV downconversion, as it absorbs radiation in the UV and re-emits at visible wavelengths. Lumogen has been used to build a white LED.[19] Because of its very high conversion efficiency, Lumogen films are used to increase the quantum efficiency of silicon-based photon detectors such as charge coupled devices (CCD's).[20–22] Lumogen coatings are also routinely applied to commercial CCD's; see, for example, Jobin Yvon Inc data sheets for front illuminated UV sensitive (FI UV) CCD's at http://www.jobinyvon.co.uk/ukdivisions/OSD/ccd_detector.htm or Princeton Instruments information on back illuminated CCD's at http://www.mso.anu.edu.au/observing/detlab/ccdlab/ccd/ccdchar/coating/unichrm.pdf. To further illustrate this application, Lumogen Yellow coatings have been used in the UV imaging systems of the Hubble Space Telescope[23] and the Cassini–Huygens Spacecraft that reached the Saturnian's system in 2004.

The NMR study of Lumogen was never reported. Its crystal structure has been determined thrice (UJOTES, UJOTES01 and UJOTES02)[24] and corresponds to **1a** (*E*,*E* configuration) (Figs 2 and 3).

Lumogen (**1**) was prepared by reacting hydrazine with 2-hydroxynaphthalene-1-carbaldehyde, a commercial compound. Lumogen can exist in three tautomeric forms: the dihydroxy

* *Correspondence to: Dolores Santa María, Departamento de Química Orgánica y Bio-Orgánica, Facultad de Ciencias, Universidad Nacional de Educación a Distancia (UNED), Senda del Rey 9, E-28040 Madrid, Spain. E-mail: dsanta@ccia.uned.es*

** *Correspondence to: Ibon Alkorta, Instituto de Química Médica, Centro de Química Orgánica 'Manuel Lora-Tamayo', IQM-CSIC, Juan de la Cierva, 3, E-28006 Madrid, Spain. E-mail: ibon@iqm.csic.es*

a *Chemistry Department and QOPNA, University of Aveiro, 3810-193 Aveiro, Portugal*

b *Departamento de Química Orgánica y Bio-Orgánica, Facultad de Ciencias, Universidad Nacional de Educación a Distancia (UNED), Senda del Rey 9, E-28040 Madrid, Spain*

c *Departamento de Física, Facultad de Ciencias Exactas y Naturales, Universidad de Buenos Aires and IFIBA, CONICET, Ciudad Universitaria, Pabellón 1, 1428 Buenos Aires, Argentina*

d *Instituto de Química Médica, Centro de Química Orgánica 'Manuel Lora-Tamayo', IQM-CSIC, Juan de la Cierva, 3, E-28006 Madrid, Spain*

azine **1a** [1,1′-(1*E*,1′*E*)-hydrazine-1,2-diylidenebis(methan-1-yl-1-ylidene)dinaphthalen-2-ol], the hydroxy-oxo hydrazone **1b** [(*Z*)-1-(((*E*)-2-((2-hydroxynaphthalen-1-yl)methylene)hydrazinyl)methylene) naphthalen-2(1*H*)-one] and the dioxo hydrazine **1c** [(1*Z*,1′*Z*)-1,1′-(hydrazine-1,2-diylbis(methan-1-yl-1-ylidene))dinaphthalen-2(1*H*)-one] (Fig. 3).

Salicylaldazine (salicylaldehyde azine) (**2**), which exists in the dihydroxy tautomeric form (Figs 4 and 5), has been much studied in photophysics. Its excited-state intramolecular proton transfer from the phenolic hydroxy group to the nitrogen of the methine bond is analogous to the fast enol → keto tautomerization of other 2-hydroxybenzenes.[25] Other salicylaldehyde azines (substituted on the phenyl ring) were studied as fluorophores,[26] for their piezochromism.[27] 2′-Hydroxyacetophenone azine (a methyl group in place of the CH) has been studied by IR and density functional theory (DFT) calculations.[28] The X-ray structure of **2** has been determined (SALIAZ, Fig. 4)[24]; the compound shows polymorphism with one form SALIAZ01, 02, 03 and 06 crystallizing in the $P2_1/n$ space group with one independent molecule and the other SALIAZ04 and 07 in the $P2_1/c$ space group with two independent molecules. We have studied the $P2_1/n$ structure (refer to the Experimental Section).

The compound can exist in three tautomeric forms similarly to Lumogen (Fig. 5). For this compound, we will discuss only the solid-state NMR results, where the tautomer present is **2a**.

On the basis of our previous experience, the *E*/*Z* isomerism about the C=N bond in aldazines derived from aromatic aldehydes such as **1** and **2** can be ruled out because the aryl group always adopts the *E* configuration. Besides, the barriers are very high (90–100 kJ mol^{-1}), and the populations do not depend on the temperature (*vide infra*) but are very sensitive to the phase.[29,30]

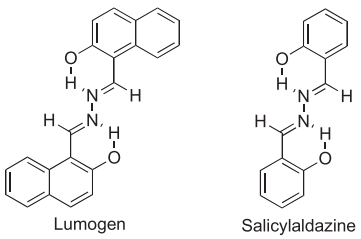

Figure 1. Structure of Lumogen (**1**) and salicylaldazine (**2**).

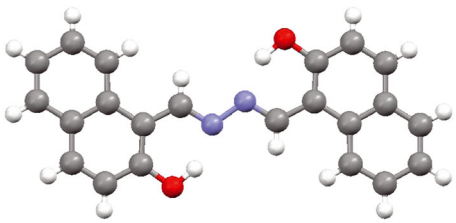

Figure 2. X-Ray crystal structure of UJOTES **1**.

Experimental Section

Chemistry

*Synthesis of 1,1′-[hydrazine-1,2-diylidenebis(methanylylidene)]bis (naphthalen-2-ol) (**1**)*

An ethanol solution (10 ml) of 2-hydroxy-1-naphthaldehyde (500 mg, 2.9 mmol) was added to a solution of hydrazinum sulfate (171.5 mg,

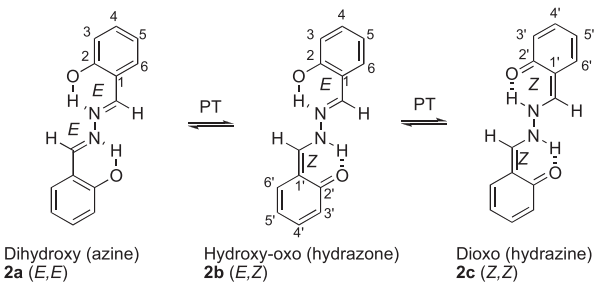

Figure 5. Tautomers of salicylaldazine (**2**).

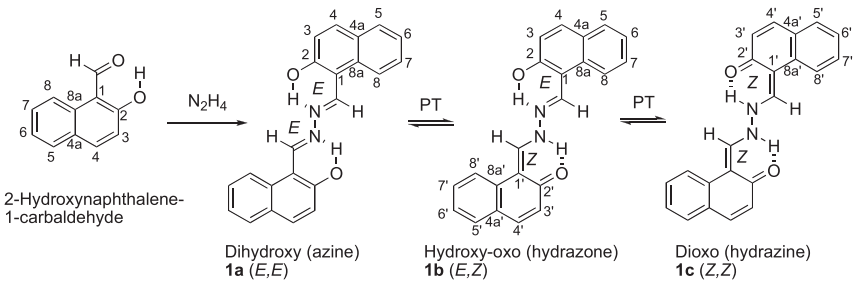

Figure 3. Tautomers (proton transfer, PT) of Lumogen (**1**).

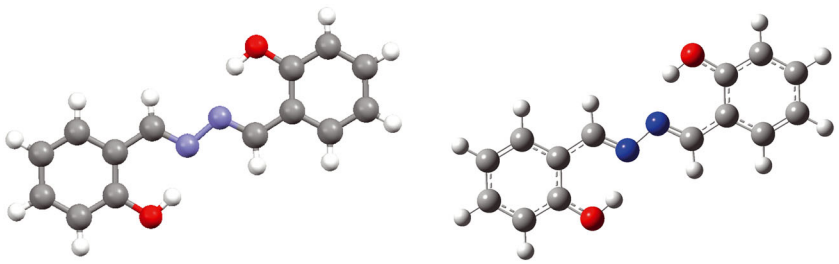

Figure 4. Left, X-Ray crystal structure of SALIAZ03 **2**; right, calculated geometry of **2a**.

1.32 mmol) in ammonia (171.6 μl). The resulting reaction mixture was stirred at room temperature under nitrogen atmosphere for a few minutes, and then it was heated at 50 °C for 4 h. After half an hour of reaction, we observed the formation of a shiny yellow precipitate. After 4 h at 50 °C, the mixture was cooled to room temperature, and the obtained solid was removed by filtration, washed with water and a small portion of ethanol and then recrystallized in ethanol. The azine was obtained as a shiny yellow solid in 60% yield, mp 309–310 °C (ethanol). Lit. 308 °C (decomp.).[31] Salicylaldazine is a commercial compound.

NMR experiments

^{1}H and ^{13}C NMR spectra were recorded on a Bruker 300 (Alfa-Aesar, referencia A10527, A Johnson Mattey Company) [300.13 MHz (^{1}H) and 75.47 MHz (^{13}C)] spectrometer with TMS as internal reference. Unequivocal ^{1}H and ^{13}C assignments were made on the basis of 2D HSQC ($^{1}H/^{13}C$) and HMBC (delays for one bond and long-range *J* C/H couplings were optimized for 145 and 7 Hz, respectively) experiments.

^{13}C (100.73 MHz) and ^{15}N (40.60 MHz) CPMAS NMR spectra have been obtained on a Bruker WB 400 spectrometer at 300 K using a 4-mm DVT probehead and a 4-mm diameter cylindrical zirconia rotor with Kel-F endcaps. Operating conditions involved 2.9 μs 90° ^{1}H pulses and decoupling field strength of 86.2 kHz by two-pulse phase modulation sequence. The non-quaternary suppression (NQS) technique to observe only the quaternary carbon atoms was employed; before the acquisition, the decoupler is switched off for a very short time of 25 μs.[32] ^{13}C spectra were originally referenced to a glycine sample, and then the chemical shifts were recalculated to the Me_4Si [for the carbonyl atom δ (glycine) = 176.1 ppm] and ^{15}N spectra to $^{15}NH_4Cl$ and then converted to nitromethane scale using the following relationship: $\delta^{15}N(\text{nitromethane}) = \delta^{15}N(\text{ammonium chloride}) - 338.1$ ppm.

Typical acquisition parameters for ^{13}C CPMAS were as follows: spectral width, 40 kHz; recycle delay, 50 s; acquisition time, 30 ms; contact time, 2 ms; and spin rate, 12 kHz. And for ^{15}N CPMAS, these were as follows: spectral width, 40 kHz; recycle delay, 50 s; acquisition time, 35 ms; contact time, 7 ms; and spin rate, 6 kHz.

X-ray powder diffraction

To check the polymorphism of salicylaldazine, we have compared the power diffraction data generated from the single-crystal structures (SALIAZ02, $P2_1/n$, vs SALIAZ07, $P2_1/c$) that are very different in the 10° to 40° 2θ region with the experimentally determined powder X-ray diffraction with our sample (Fig. 6). There is no doubt that our sample corresponds to SALIAZ02.

Computational details

Geometries of the different structures of compound **1** were fully optimized at the B3LYP theoretical level,[33,34] with the 6-311++G (d,p) basis set[35] as implemented in the Gaussian 03 program.[36] Harmonic frequency calculations[37] verified the nature of the stationary points as minima (all real frequencies). ^{13}C and ^{15}N absolute shieldings of compounds **1a–1c** have been calculated over the fully optimized geometries within the gauge-including atomic orbitals (GIAO) approximation.[38,39] Polarizable continuum model (PCM) calculations[40] were used as implemented in Gaussian 03.

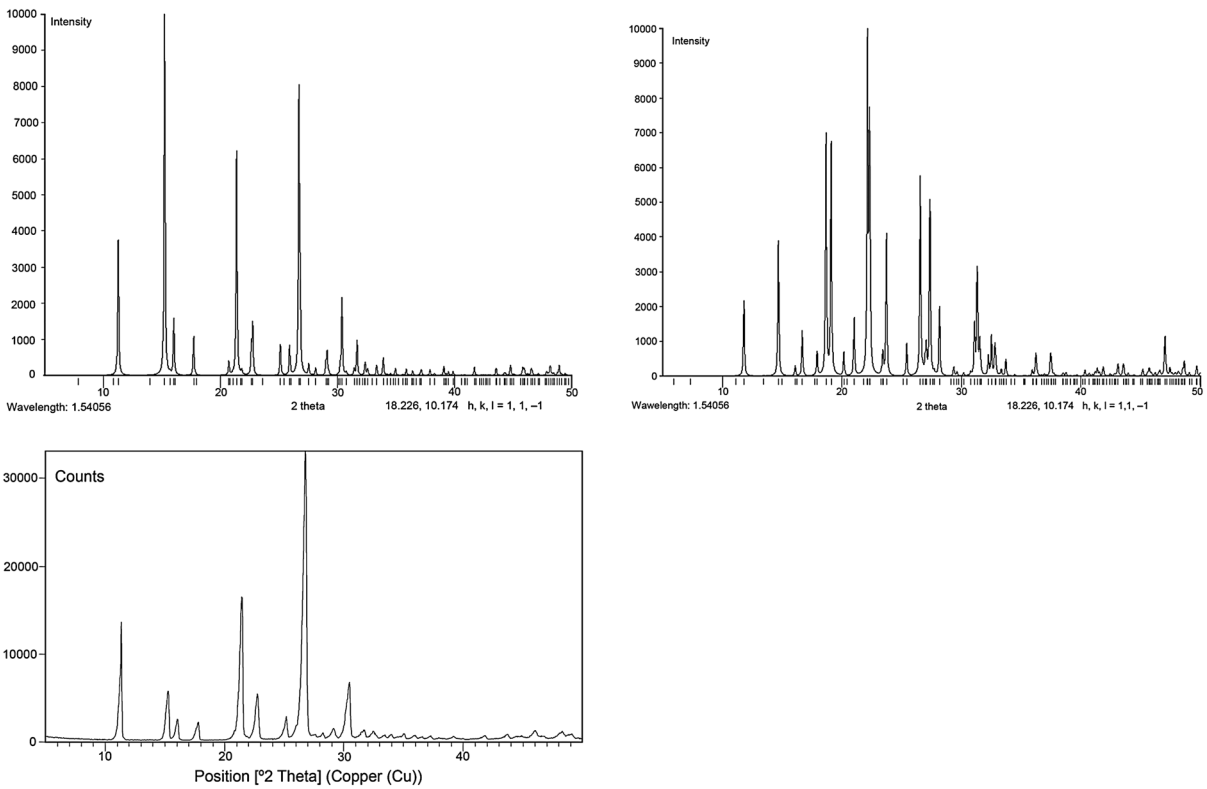

Figure 6. The two polymorphs of salicylaldazine: top left, SALIAZ02, $P2_1/n$, one independent molecule; top right, SALIAZ07, $P2_1/c$, two independent molecules; bottom, experimental X-ray powder diffraction.

The absolute shieldings (σ, ppm) were transformed into chemical shifts (δ, ppm) by means of the following empirical equations.

$$\delta^{1}H = 31.0–0.97\sigma^{1}H. \text{ [17]} \quad (1)$$

$$\delta^{13}C = 175.7–0.963\sigma^{13}C. \text{ [41]} \quad (2)$$

$$\delta^{15}N = -152.0–0.946\sigma^{15}N. \text{ [41]} \quad (3)$$

These equations were established using a large collection of data and relate the calculated values for the gas phase with experimental values determined in solution and in the solid state [only (2) and (3)].[42] For this reason, GIAO calculations over PCM solvated molecules do not improve considerably the results. However, as we will show further on, in the present case, GIAO/PCM/MSO explains better certain ^{13}C chemical shifts.

Quantum ESPRESSO (QE)[43] was employed to optimize the crystal and the isolated molecule structures, using DFT-D.[44–46] The DFT gauge-including projector augmented wave (GIPAW) method with pseudopotentials to approximate the core electron wavefunction, as implemented in the program *Quantum ESPRESSO*, is used to predict the complete ^{13}C chemical shift tensors for all carbons and, for both configurations, crystal and isolated molecule, at the same level of theory, *PBE*.[47,48]

The parameters employed to make QE calculations were set to achieve convergence in the Self consistent field (SCF) energy. The details of their selection are the following. (i) The DFT-D pseudopotentials from www.quantum-espresso.org are the norm-conserving *pbe-tm-gipaw* and the ultrasoft *pbe-rrjkus-gipaw-dc*, and both of them were tested for every calculation. (ii) The convergence of the SCF calculations, *conv*, was varied from 10^{-7} to 10^{-12} and set in 10^{-10}. (iii) The energy cutoff for the wavefunction, *ecutwfc*, was varied between 35 and 95 and set in 65, corresponding to the minimum number of plane waves to achieve SCF energy convergence. (iv) The *k* points were varied between 1 and 4 in each dimension and set in $k = 2$, employing again the criteria of reaching the minimum SCF energy.

All calculations were performed using version 5.0.1 of QE. Calculations were performed on four-core nodes (Intel I5 processors, 3.0 GHz) with 16 GB RAM.

Results and Discussion

Theoretical part: Lumogen – energies and geometries

We have reported in Table 1 the free energy results concerning the three tautomers of Lumogen.

According to the calculations, in gas phase, only tautomer **1a** should be present, whereas in dimethyl sulfoxide (DMSO) at 20 °C, 1.8% of tautomer **1b** should accompany the major one. Taking into account that there are two identical tautomers, **1b** and **1b′**, the proportion of the minor isomer should be 3.6%. In neither case, the very unstable tautomer **1c** should be observed. Because the single N–N bond isolated both moieties, Lumogen should, in a first approximation, behave as two independent parts, i.e. tautomer **1b** should be intermediate in energy relative to tautomers **1a** and **1c**, 27.0 kJ mol^{-1} in the gas phase and 20.8 kJ mol^{-1} in DMSO. Actually, it is more stable by 11.1 mol^{-1}, showing that the tautomerism of one half influence the tautomerism of the other half.

The structures corresponding to **1a**, **1b** and **1c** are represented in Fig. 7.

The calculated geometry of tautomer **1a** is almost identical to that determined by X-ray crystallography (UJOTES **1**, Fig. 1). Tautomer **1b** is in the way between **1a** and **1c**, with two identical transition states.

Theoretical part: salicylaldazine – geometries

The structure corresponding to **2a** is represented in Fig. 4 right; the near identity of both structures is apparent.

NMR part: Lumogen – solution and solid-state results

In solution, the existence of two structures is observed in ^{1}H as well in ^{13}C NMR in the form of narrow signals. This means that the oxo/hydroxy tautomerization barrier is high in the NMR time scale and that, if tautomer **1b** is present, the signals from both halves, the hydroxy and oxo, should be observed.

The ^{1}H NMR spectrum of Lumogen **1** at room temperature (20 °C) shows the signals of two structures, in a proportion of 60.9 : 39.1. To obtain some information about these structures and to fully characterize each of them, we acquired ^{1}H NMR spectra at different temperatures. At 80 °C, we observed almost only one structure (81.6%), and we run all the necessary spectra for their characterization. The protonated carbon assignment were mainly based on the HSQC spectrum and confirmed by some long-range connectivities found in the HMBC spectrum. This spectrum allowed the unequivocal assignment of the non-protonated carbons (Fig. 8A).

At room temperature (20 °C), the signals of structures **1a** and **1b** can be seen. The percentage of each of the structures are based on the integrals of the N=CH (s, 10.00 ppm) and OH (s br, 12.88 ppm) of **1a** and of the NHC*H* (s, 10.82 ppm) and N*H*CH (brs, 12.01 ppm) of **1b**. In the spectrum at 10 °C, the proportion changed to 56.2 : 43.8. At this temperature, we have also unequivocally assigned all the proton and carbon resonances through HSQC and HMBC spectra. We have also carried out a NOESY

Table 1. Absolute free energies (hartree), relative free energies (kJ mol^{-1}), equilibrium constants at 20 °C and dipole moments (D) for the gas phase and DMSO solution (PCM); B3LYP/6-311++G(d,p) calculations

Compound	Phase	ΔG	ΔG_{rel}	K	μ
1a	Gas	−1107.94350	0.0	1	0.00
1b	Gas	−1107.93744	15.9	1.46×10^{-3}	1.44
1c	Gas	−1107.92298	53.9	—	0.46
1a	DMSO	−1107.95457	0.0	1	0.00
1b	DMSO	−1107.95086	9.7	1.84×10^{-2}	2.50
1c	DMSO	−1107.93871	41.6	—	0.65

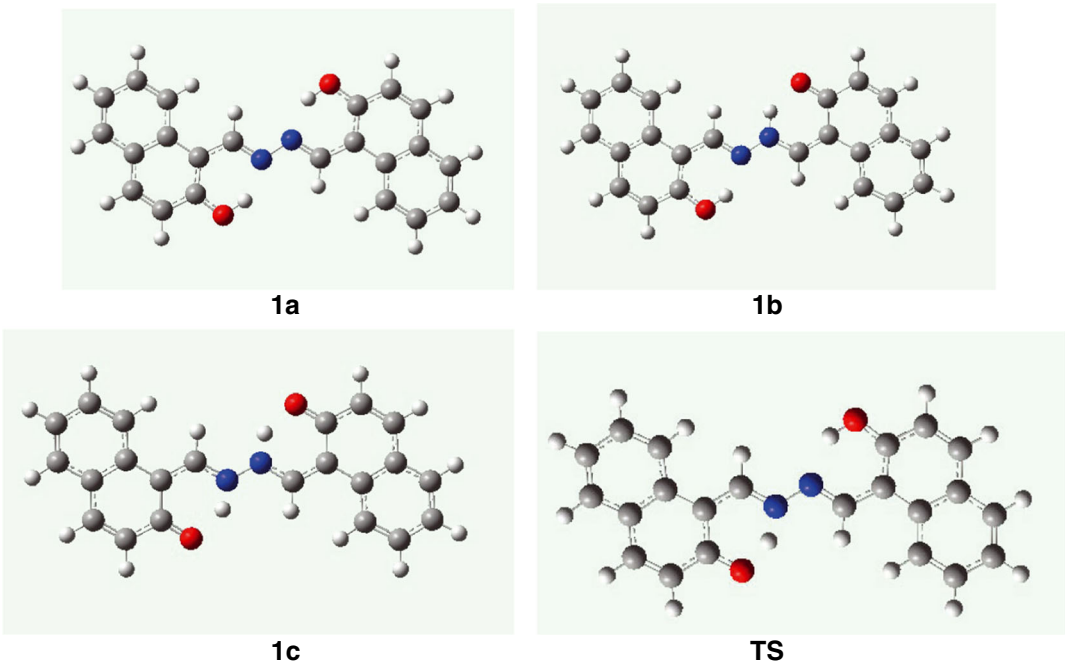

Figure 7. A view of the optimized geometries of tautomers **1a**, **1b** and **1c** and the Transition state (TS) between **1a** and **1b**.

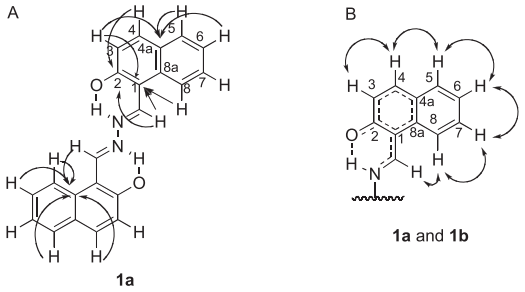

Figure 8. (A) Main connectivities observed in the HMBC spectrum (80 °C) of the structure **1a**; (B) NOE cross peaks observed in the NOESY spectrum of **1a** and **1b** at 10 °C.

spectra to confirm the proton assignments of both structures and also to establish their stereospatial relationships (Fig. 8B).

Lumogen is very insoluble at the concentrations required for NMR even for high-field spectrometers. Among the usual deuterated solvents, the only useful one is deuterated DMSO (DMSO-d_6). In ^{1}H NMR at room temperature (20 °C), there are the signals corresponding to two tautomers. Then, when the solution was heated, the presence of the minor tautomer almost disappears. On the other hand, decreasing the temperature increases the population of the minor tautomer. The percentages reported in Table 2 correspond to the ^{1}H NMR integrals.

Note that the population of the minor isomer decreases when the temperature increases, from 43.8% at 10 °C to 18.4% at 80 °C. When we insert these values into the $\Delta G_T = -RT\ \mathrm{Ln}\ K_T$ equation ($R = 8.3145\ \mathrm{J\,mol^{-1}\,K^{-1}}$), the relationship is linear ($R^2 = 0.999$), and using the ΔG_T values to obtain ΔH_T and ΔS_T ($\Delta G_T = \Delta H_T - T\Delta S_T$) leads to $\Delta H_T = -(14.8 \pm 0.2)\ \mathrm{kJ\,mol^{-1}}$ and $\Delta S_T = (54.3 \pm 0.8)\ \mathrm{J\,K^{-1}}$. Note that in Table 1, $\Delta G_{rel} = 9.7\ \mathrm{kJ\,mol^{-1}}$, a larger difference than the results reported in Table 2.

Table 2. Variation of the populations of both isomers with the temperature; we have defined $K_T = [\mathbf{1b}]/[\mathbf{1a}]$

Temperature		Major	Minor	K_T (minor/major)	Ln K_T	ΔG_T
°C	*K*	**1a**	**1b/1b′**			
80	353.15	81.6	18.4	0.225	−1.489	4.374
60	333.15	76.5	23.5	0.307	−1.180	3.269
40	313.15	69.3	30.7	0.443	−0.814	2.120
20	293.15	60.9	39.1	0.642	−0.443	1.080
10	283.15	56.2	43.8	0.779	−0.249	0.587

The ^{1}H and ^{13}C chemical shifts vary slightly with the temperature (Tables 3 and 4).

In the solid state, the structure of Lumogen as determined by diffraction is **1a** (Fig. 1). Its ^{13}C and ^{15}N CPMAS spectra are reported in Figs. 9 and 10.

The accidental coincidence of the C2 (q) and the CH at 161.9 ppm was verified recording the NQS: the quaternary carbons appear at 108.3 (C1), 128.6 (C4a), 133.7 (C8a) and 161.9 ppm (C2). Another CPMAS experiment was carried out with contact times of 200 μs instead of 2 ms resulting in a spectrum where the quaternary carbons disappear or are very small.

An NQS sequence was used to ascertain that the quaternary carbons are C1 (117.9 ppm) and C2 (160.2 ppm) (Fig. 11). The difference in ^{15}N chemical shifts, −9.4 ppm (−58.3 ppm, Fig. 10, and −48.9 ppm, Fig. 12), corresponds to calculated values of −63.4 **1a** and −55.2 ppm **1**, i.e. −8.2 ppm.

Comparison of calculated and experimental chemical shifts: identification of the tautomers of Lumogen 1 in solution

We have carried out ^{13}C GIAO/B3LYP/6-311++G(d,p) calculations of the three tautomers of **1** in the gas phase and in DMSO (PCM) (Table 5).

Table 3. ^{1}H chemical shifts (ppm) and some ^{1}H–^{1}H SSCC (Hz) in DMSO-d_6

	Temperature (°C)				
	80°		20°		10°
	Major **1a**	Major **1a**	Minor **1b**	Major **1a**	Minor **1b**
	(81.6%)	(60.9%)	(39.1%)	(56.2%)	(43.8%)
H3	7.27, d	7.30, d	7.25, d	7.36, d	7.31, d
	J = 9.0	J = 9.0	J = 9.1	J = 9.1	J = 9.0
H4	8.01, d	8.05, d	8.15, d	8.12, d	8.21, d
	J = 9.0	J = 9.0	J = 9.1	J = 9.1	J = 9.0
H5	7.90, dd	7.93, d	7.90, d	7.93, d	7.96, d
	J = 8.0, 1.4	J = 7.9, 1.2	J = 8.6	J = 8.0	J = 8.2
H6	7.44, ddd,	7.45, dd	7.45	7.52, m	7.50, m
	J = 1.0, 7.0, 8.0	J = 6.9, 7.9	under the major		
H7	7.62, ddd,	7.63, ddd	7.63	7.69, m	7.69, m
	J = 1.4. 7.0, 8.5	J = 1.2. 6.9, 8.5	under the major		
H8	8.58, d,	8.65, d	8.93, d	8.71, d	9.01, d
	J = 8.5	J = 8.5	J = 8.8	J = 8.9	J = 8.7
CH	9.86, s	10.00, s	10.82, s	10.08, s	10.87, s
XH	12.65, brs, OH	12.88, brs, OH	12.01, brs, NH/OH	13.00, brs, OH	12.15, brs, NH/OH

Table 4. ^{13}C chemical shifts (ppm) in DMSO-d_6; in the last column, the ^{13}C CPMAS results are reported

	Major **1a**	Minor **1b**	CPMAS
	80 °C	10 °C	r.t.
C1	108.3	108.3	108.3
C2	159.7	159.7	161.9
C3	118.5	118.5	120.9
C4	134.3	134.3	133.7
C4a	128.5	128.5	128.6
C5	128.5	128.5	128.6
C6	123.5	123.5	124.6
C7	127.6	127.6	128.6
C8	121.3	121.3	120.9
C8a	132.1	132.1	133.7
CH	160.4	160.4	161.9
C1′	—	112.6	
C2′	—	193.1	
C3′	—	129.1	
C4′	—	138.8	
C4a′	—	129.7	
C5′	—	129.1	
C6′	—	124.6	
C7′	—	127.8	
C8′	—	122.5	
C8a′	—	131.9	
CH′	—	164.3	

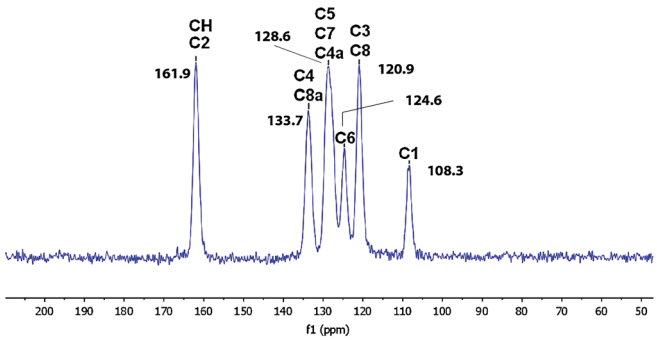

Figure 9. ^{13}C CPMAS NMR spectrum of Lumogen (spectral width, 40 kHz; recycle delay, 50 s; acquisition time, 30 ms; contact time, 2 ms; scans, 365; and spin rate, 12 kHz).

To decide between different options concerning the tautomers, we have compared the experimental ^{13}C chemical shifts of Tables 3 and 4 (both DMSO-d_6 and CPMAS) with the calculated values of Table 5 (both gas and DMSO-d_6) for the three possible tautomers **1a**, **1b** and **1c**. To do this, we have calculated different regression equations to select the better ones. Besides the correlation coefficient (R^2 values, which also is reflected in the error of the parameters), it is important to have an intercept close to 0 and a slope close to 1. We have reported in Table 6 the results we have obtained.

i. There is no doubt that the major tautomer is **1a** because the agreement is very good; refer to Eqns (4a) and (4b), the $GIAO_{DMSO}$ values being a little better (0.99 vs 0.98 and a smaller intercept). The worse point corresponds to the CH, which appears experimentally at 160.4 ppm, whereas the fitted value according to Eqn (4a) is 156.0 ppm and according to Eqn (4b) 157.1 ppm.
ii. On the basis of energy calculations and the simple considerations we discussed previously, we consider that the minor isomer is **1b**. We have assumed that the signals corresponding to the hydroxy part of tautomer **1b** are identical to those of **1a** (again, the $GIAO_{DMSO}$ values are a little better). An examination of the ^{13}C calculated values shows that this is indeed the case save for the CHs (156.9 and 146.2 ppm) [the same happens for the CHs of the oxo part between **1b** and **1c**

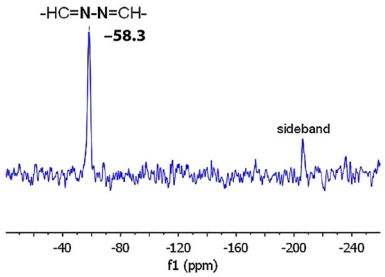

Figure 10. ^{15}N CPMAS NMR spectrum of Lumogen (spectral width, 40 kHz; recycle delay, 50 s; acquisition time, 35 ms; contact time, 7 ms; scans, 7086; and spin rate, 6 kHz).

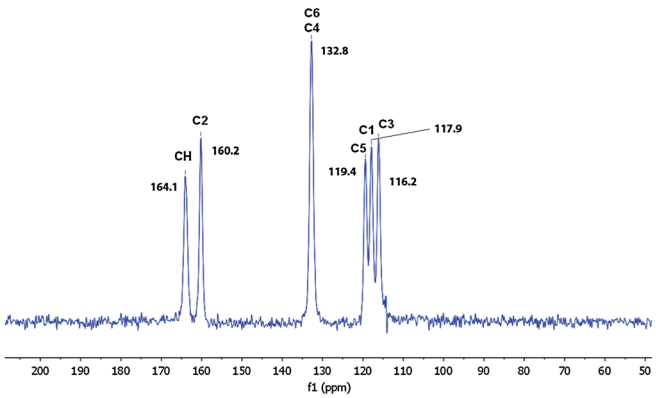

Figure 11. ^{13}C CPMAS NMR spectrum of salicylaldazine (spectral width, 40 kHz; recycle delay, 50 s; acquisition time, 30 ms; contact time, 2 ms; scans, 365; and spin rate, 12 kHz).

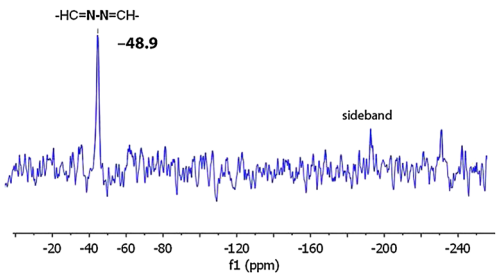

Figure 12. ^{15}N CPMAS NMR spectrum of salicylaldazine (spectral width, 40 kHz; recycle delay, 50 s; acquisition time, 35 ms; contact time, 7 ms; scans, 1329; and spin rate, 6 kHz).

(144.2 and 140.2 ppm)]. A first regression with all the values of **1a** and **1b** leads to Eqns (5a) and (5b).

An examination of the residuals shows that the largest deviations correspond to the CHs of the bridge of **1b**. Introducing a dummy variable for these two ^{13}C signals leads to Eqns (6a) and (6b). The dummies are very important (16.2 and 13.8 ppm, depending on the calculations being gas phase or DMSO, respectively).

On the other hand, if we suppose that the signals of the oxo part of **1b** belong to **1c**, Eqns (7a) and (7b) without dummies and Eqns (8a) and (8b) with dummies are obtained.

Considering that the number of points is larger [for instance, there are two CHs in Eqns (6a) and (6b) and only one in Eqns (8a) and (8b)] and that the correlation coefficients are slightly lower, we conclude that the minor isomer is **1b**.

Table 5. ^{13}C calculated chemical shifts (ppm)

Atom	Gas			DMSO		
	1a	**1b**	**1c**	**1a**	**1b**	**1c**
C1	108.2	108.3	—	109.1	108.6	—
C2	163.7	162.2	—	163.3	161.6	—
C3	118.9	118.9	—	118.8	118.5	—
C4	134.5	134.2	—	136.7	135.4	—
C4a	128.0	128.3	—	128.4	128.7	—
C5	128.9	129.3	—	130.2	129.5	—
C6	123.1	123.2	—	124.1	124.2	—
C7	128.8	128.6	—	129.3	129.7	—
C8	118.2	117.4	—	119.0	118.3	—
C8a	134.4	132.5	—	133.4	133.3	—
CH	156.9	146.2	—	158.6	149.0	—
C1′	—	107.4	106.7	—	107.4	106.5
C2′	—	182.4	180.6	—	182.5	181.4
C3′	—	127.4	125.8	—	126.5	125.4
C4′	—	139.6	138.9	—	140.6	141.0
C4a′	—	126.3	126.6	—	126.8	127.2
C5′	—	129.3	129.3	—	129.6	130.0
C6′	—	122.8	122.4	—	123.2	123.3
C7′	—	128.1	128.7	—	130.0	129.4
C8′	—	116.2	115.9	—	116.7	117.3
C8a′	—	134.5	133.8	—	135.3	134.7
CH′	—	144.2	140.2	—	147.2	142.2

iii. It appears that the structure of **1a** is as represented with both its O–H···N HBs intact in DMSO. On the other hand, the structure of **1b** has probably the weaker N–H···O HBs partially broken in DMSO, explaining the anomalies of the Ar-**C**H=N carbon atoms.

iv. The data of Fig. 9 (solid state) agree with the values in DMSO-d_6 for tautomer **1a** and with the calculated values [Eqns (9a) and (9b)]. The worse point corresponds to the CH. In this case, the use of DMSO calculated values does not improve the correlations.

v. The calculated ^{15}N chemical shifts are −62.0 ppm for **1a**, −201.3 and −93.7 ppm for **1b** and −219.4 ppm for **1c**. As expected for tautomerism involving N atoms, ^{15}N NMR is the method of choice, but in solution for insoluble compounds, ^{15}N labeling is compulsory.

The anomaly of carbons CH and C2 of Lumogen and salicylaldazine

We have already encountered the problem of the CH that needs an empirical correction (dummy). The second worse points in the equations of Table 6 correspond to the C2. We will examine in this section the problem of these signals in compounds **1a** and **2a** (dihydroxy tautomers, the only present in the solid state).

The use of PCM–DMSO calculated ^{13}C chemical shifts of **1** partly corrects the anomalies found in the gas phase both in solution and in the solid state between 25% and 30%, but still the agreement is not satisfying.

We then checked if the anomalies are found in salicylaldazine (Table 7). We have used the equations devised for Lumogen [Eqns (4a), (4b), (9a) and (9b)] to predict the experimental values and to calculate the residuals.

Table 6. Different regression equations for ^{13}C NMR chemical shifts (δ, ppm)

Eqn	Conditions	Method	Intercept	Slope	Number of points	R^2
4a	$DMSO_{major}$	$GIAO_{gas}$ **1a**	(4.2 ± 5.6)	(0.97 ± 0.04)	11	0.98
4b	$DMSO_{major}$	$GIAO_{DMSO}$ **1a**	(2.9 ± 4.5)	(0.97 ± 0.03)	11	0.99
5a	$DMSO_{maj+min}$	$GIAO_{gas}$ **1a** + **1b**	−(6.4 ± 7.0)	(1.06 ± 0.05)	33	0.93
5b	$DMSO_{maj+min}$	$GIAO_{DMSO}$ **1a** + **1b**	−(7.4 ± 7.0)	(1.06 ± 0.05)	33	0.94
6a	$DMSO_{maj+min}$	$GIAO_{gas}$ **1a** + **1b**	−(0.5 ± 4.4)	(1.01 ± 0.03)		
		Dummy		(16.2 ± 2.3)	33	0.98
6b	$DMSO_{maj+min}$	$GIAO_{DMSO}$ **1a** + **1b**	−(1.4 ± 4.5)	(1.01 ± 0.03)		
		Dummy	(13.8 ± 2.3)		33	0.98
7a	$DMSO_{minor}$	$GIAO_{gas}$ **1a**	−(13.8 ± 16.7)	(1.1 ± 0.1)	11	0.90
7b	$DMSO_{minor}$	$GIAO_{DMSO}$ **1a**	−(13.2 ± 16.2)	(1.1 ± 0.1)	11	0.91
8a	$DMSO_{maj+min}$	$GIAO_{gas}$ **1a** + **1b**	−(9.3 ± 9.4)	(1.09 ± 0.07)		
		Dummy		(20.2 ± 4.4)	11	0.96
8b	$DMSO_{maj+min}$	$GIAO_{DMSO}$ **1a** + **1b**	−(8.3 ± 9.4)	(1.08 ± 0.08)		
		Dummy	(18.9 ± 4.8)		11	0.96
9a	CPMAS	$GIAO_{gas}$ **1a**	(1.2 ± 5.2)	(1.00 ± 0.04)	11	0.99
9b	CPMAS	$GIAO_{DMSO}$ **1a**	(0.3 ± 5.0)	(1.00 ± 0.04)	11	0.99

Table 7. The problem of the signals of the carbon atoms involved in the HB

Mol.	Exp. DMSO	Exp. CPMAS	Calc. gas	Calc. DMSO	Eqn	Residual	Fitted
1a C2	159.7	—	163.7	—	4a	−2.9	162.6
1a CH	160.4	—	156.9	—	4a	+4.4	156.0
1a C2	159.7	—	—	163.3	4b	−2.0	161.7
1a CH	160.4	—	158.6	4b	+3.3	157.1	
1a C2	—	161.9	163.7	—	9a	−2.4	164.3
1a CH	—	161.9	156.9	—	9a	+4.4	157.5
1a C2	—	161.9	163.3	9b	−1.4	163.3	
1a CH	—	161.9	158.6	9b	+3.3	158.6	
						Difference	Predicted
2a C2	159.7	—	163.1	—	4a′	−2.3	162.0
2a CH	164.6	—	162.6	—	4a′	+3.1	161.5
2a C2	159.7	—	—	162.3	4b′	−1.0	160.7
2a CH	164.6	—	—	164.3	4b′	+1.9	162.7
2a C2	—	160.2	163.1	—	9a′	−3.5	163.7
2a CH	—	164.1	162.6	—	9a′	+0.9	163.2
2a C2	—	160.2	—	162.3	9b′	−2.1	162.3
2a CH	—	164.1	—	164.3	9b′	0.0	164.3

Comparison of GIAO/DFT with GIPAW calculations

To this point, all our calculations were made on an isolated molecule, in the gas phase or surrounded by a continuum with the dielectric properties of DMSO. We want in this part of our paper to compare the CPMAS data of **1a** and **2a** with the σ calculated values using the GIPAW DFT-D method (refer to the Computational Details Section). The calculations for the crystal structures employing pbe-rrjkus-gipaw-dc are indicated as PBE-crystal-rrjkus and PBE-mol-rrjkus for the configurations of crystal and isolated molecule, respectively. Correspondingly, PBE-crystal-tm and PBE-mol-tm indicate calculations using the norm-conserving pbe-tm-gipaw. As it is indicated in the Computational Details Section, all the systems have been optimized with QE at the same level of theory, pbe-rrjkus-gipaw-dc and pbe-tm-gipaw. The data are reported in Table 8.

The statistical treatments of these data are reported in Table 9. Several conclusions can be drawn from Table 9.

1. When the data of **1a** and **2a** are put together, the anomaly of C2 disappears, other atoms showing larger deviations.
2. The errors concerning the CH of **2a** are much lower and are not significantly different from other atoms.
3. In what concerns the CPMAS experimental results, according to the R^2 values, GIPAW does not improve the gas-phase calculations.
4. The anomaly concerning the CH of **1a** is not corrected by the GIPAW calculations.
5. The DMSO cavity simulates the solid state. This is not surprising because an isolated molecule in a DMSO cavity shows some similarity with a molecule surrounded by other identical molecules.

Table 8. Comparison of different approaches to calculated solid-state absolute shieldings (ppm); experimental values in δ (ppm)

Atom	Exp.	GIAO gas	GIAO DMSO	PBE-crystal-rrjkus	PBE-crystal-tm	PBE-mol-rrjkus	PBE-mol-tm
C1 L	108.3	70.08	69.20	57.89	58.18	60.13	55.67
C2 L	161.9	12.44	12.92	0.75	0.66	1.76	−4.13
C3 L	120.9	59.01	59.12	46.91	47.47	51.33	47.73
C4 L	133.7	42.80	40.49	33.24	33.39	34.35	30.87
C4a L	128.6	49.50	49.13	40.02	40.07	41.26	36.91
C5 L	128.6	48.61	47.28	38.12	38.43	41.53	38.11
C6 L	124.6	54.60	53.60	45.52	45.76	48.19	44.30
C7 L	128.6	48.70	48.18	41.65	41.79	41.98	38.20
C8 L	120.9	59.73	58.82	49.45	49.39	50.16	46.56
C8a L	133.7	42.94	43.91	35.16	35.12	36.38	32.32
CH L	161.9	19.48	17.77	11.34	11.36	13.34	8.18
C1 S	117.9	60.24	59.67	49.25	44.89	49.75	45.43
C2 S	160.2	13.04	13.91	5.87	0.52	4.20	−1.21
C3 S	116.2	60.72	61.47	51.15	46.71	51.22	46.92
C4 S	132.8	43.86	42.90	36.38	32.66	36.16	32.30
C5 S	119.4	59.70	58.42	52.05	48.32	52.32	48.58
C6 S	132.8	44.64	43.17	34.57	30.60	35.05	31.38
CH S	164.1	13.58	11.90	2.14	−3.25	1.97	−3.59

L, Lumogen; S, salicylaldazine.

Table 9. Regression analysis (the experimental value of CH L is 161.9 ppm); the data for 17 points correspond to a set where the CH of Lumogen has been removed

Method	R^2	Worse atom	CH L error	CH L fitted	Intercept	Slope
18 points						
GIAO gas	0.990	CH L	+4.9	157.0	(175.4 ± 1.2)	−(0.95 ± 0.02)
GIAO DMSO	0.992	CH L	+3.9	158.0	(174.9 ± 1.0)	−(0.95 ± 0.02)
PBE-crystal-rrjkus	0.983	CH L	+6.1	155.8	(166.6 ± 1.2)	−(0.96 ± 0.03)
PBE-crystal-tm	0.965	CH L	+8.6	153.3	(163.7 ± 1.7)	−(0.92 ± 0.04)
PBE-mol-rrjkus	0.978	CH L	+7.7	154.2	(166.6 ± 1.4)	−(0.93 ± 0.04)
PBE-mol-tm	0.975	CH L	+7.6	154.3	(161.7 ± 1.3)	−(0.90 ± 0.04)
17 points						
GIAO gas	0.994	CH S	+2.7	(173.9 ± 0.9)	−(0.92 ± 0.02)	
GIAO DMSO	0.995	C3 L	+2.4	(173.7 ± 0.8)	−(0.93 ± 0.02)	
PBE-crystal-rrjkus	0.989	C1 L	−3.3	(165.1 ± 1.0)	−(0.92 ± 0.02)	
PBE-crystal-tm	0.978	C3 S	−4.7	(161.8 ± 1.3)	−(0.88 ± 0.03)	
PBE-mol-rrjkus	0.989	C1 L	−2.9	(164.8 ± 1.0)	−(0.89 ± 0.02)	
PBE-mol-tm	0.986	C1 L	−3.8	(160.1 ± 1.0)	−(0.86 ± 0.03)	

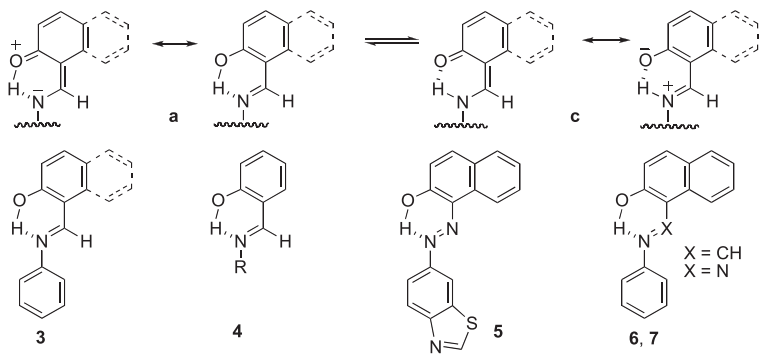

Figure 13. Related systems.

6. PCM calculations using water instead of DMSO do not improve the results (all the values of Table 9 for DMSO remains almost unchanged).

Conclusions

The azines studied in this paper belong to a series of compounds related to the Bertolasi and Gilli's resonance-assisted hydrogen bond concept, i.e. π-bond cooperativity (or synergic interplay between π-delocalization and H-bond strengthening).[49] Some examples are reported in Fig. 13, most of them concerning Schiff bases, which can be viewed as 'half-azines'.

The Schiff base **3** was studied by NMR concluding that only the OH tautomer **a** was present.[50–52] More recently, Potrzebowski *et al*. reported the case of two very similar Schiff bases one existing in the conventional phenol-imine tautomer **a** and the other in the less usual keto-amine tautomer **c** (there is an OH group *ortho* to the carbonyl).[53] Compound **4** was also studied by NMR concluding that both tautomers **a** and **c** were present.[54] The same conclusion was reported for derivative **5**.[55]

A series of papers deal with naphthalene derivatives **6** (a Schiff base) and **7** (an azo compound); by using NMR, the proportion of both tautomers was established[51,56] (in the solid state only, tautomer **a** was present)[57]; electronic spectra were used to determine the thermodynamic parameters. In the case of **5**, they were $\Delta H_T = -2.5\ kJ\ mol^{-1}$, $\Delta H_T = -9.1\ J\ mol^{-1}\ K^{-1}$ (ethanol) and $\Delta H_T = -0.8\ kJ\ mol^{-1}$, $\Delta H_T = -22.7\ J\ mol^{-1}\ K^{-1}$ (methylcyclohexane/toluene).[58,59] Note that their ΔH_T values have the same sign but lower absolute values than ours ($-14.8\ kJ\ mol^{-1}$). On the other hand, our ΔS_T is much larger ($+54.4\ J\ mol^{-1}\ K^{-1}$) and of the opposite sign to those reported in Fig. 13.

The dipolar resonance forms of Fig. 13 could explain the anomalies of the signals of carbon atoms involved in the pseudo six-membered ring (CH, C1 and C2) modifying the position of the proton involved in the HB. This has been demonstrated for Schiff bases by Potrzebowski *et al*.[53] These authors carried out a series of calculations moving the H along the intramolecular HB finding that its positions is determinant to explain the experimental results. Previous results in this line were reported by Limbach *et al*.[60,61]

All the studies based on NMR (chemical shifts, coupling constants, deuterium-induced chemical shifts differences and others) are based on average signals and interpolation methods that need values for both tautomers usually corresponding to model compounds.[62] Here, for the first time, the signals of both tautomers were observed in solution, and the tautomeric equilibrium constant directly measured. Our results may be useful to help understanding the case of more complex situations such as of the azo-hydrazone tautomerism of C_3-symmetric trisazo dyes[63] and other dyes,[64] as well as the effect of protonation,[65,66] complexation with metals[67,68] and excited states,[69,70] over the equilibria discussed in the present paper.

Acknowledgements

Thanks are given to the Ministerio de Economía y Competitividad of Spain (Projects CTQ2012-35513-C02-02 and CTQ2010-16122) and the Comunidad Autónoma de Madrid (Project MADRISOLAR2, ref. S2009/PPQ-1533). Financial support from CONICET and Universidad de Buenos Aires are gratefully acknowledged. We thank Dr Ulises Acuña (Instituto de Química Física 'Rocasolano', CSIC, for suggesting the study of Lumogen.

References

[1] E. Arnal, J. Elguero, R. Jacquier, C. Marzin, J. Wilde. *Bull. Soc. Chim. Fr.* **1966**, 877.
[2] J. Elguero, R. Jacquier, C. Marzin. *Bull. Soc. Chim. Fr.* **1966**, 2132.
[3] J. Elguero, R. Jacquier, C. Marzin. *Bull. Soc. Chim. Fr.* **1966**, 3005.
[4] J. Berthou, J. Elguero, R. Jacquier, C. Marzin, C. Rérat. *Compt. Rend. Acad. Sci. (Paris)* **1967**, *265C*, 513.
[5] J. Elguero, R. Jacquier, C. Marzin. *Bull. Soc. Chim. Fr.* **1968**, 713.
[6] J. Elguero, R. Jacquier, C. Marzin. *Bull. Soc. Chim. Fr.* **1969**, 1367.
[7] J. Elguero, R. Jacquier, C. Marzin. *Bull. Soc. Chim. Fr.* **1969**, 1374.
[8] V. Tabacik, V. Pellegrin, J. Elguero, R. Jacquier, C. Marzin. *J. Mol. Struct.* **1971**, *8*, 173.
[9] J. Elguero, C. Marzin, J. Berthou. *Bull. Soc. Chim. Fr.* **1973**, 3303.
[10] D. Sanz, M. A. Ponce, R. M. Claramunt, C. Fernández-Castaño, C. Foces-Foces, J. Elguero. *J. Phys. Org. Chem.* **1999**, *12*, 455.
[11] M. Marcos, E. Meléndez, J. L. Serrano, J. Elguero, R. Phan Tan Luu, D. Mathieu. *An. Quim.* **1983**, *79B*, 664.
[12] M. Marcos, E. Meléndez, J. L. Serrano, D. Mathieu, R. Phan Tan Luu, J. Elguero. *Bull. Soc. Chim. Belg.* **1983**, *92*, 429.
[13] J. L. Serrano, M. Marcos, E. Meléndez, C. Albano, S. Wold, J. Elguero. *Acta Chem. Scand.* **1985**, *B39*, 329.
[14] J. Elguero, C. Jaime, M. Marcos, E. Meléndez, F. Sánchez-Ferrando, J. L. Serrano. *J. Mol. Struct. (THEOCHEM)* **1987**, *150*, 1.
[15] F. Blanco, I. Alkorta, J. Elguero. *J. Mol. Struct. (THEOCHEM)* **2007**, *847*, 25.
[16] I. Alkorta, F. Blanco, J. Elguero. *Arkivoc* **2008**, *vii*, 48.
[17] A. M. S. Silva, R. M. S. Sousa, M. L. Jimeno, F. Blanco, I. Alkorta, J. Elguero. *Magn. Reson. Chem.* **2008**, *46*, 859.
[18] F. Blanco, I. Alkorta, J. Elguero. *Croat. Chem. Acta* **2009**, *82*, 173.
[19] S. C. Allen, A. J. Steckl. *Appl. Phys. Lett.* **2008**, *92*, 143309.
[20] J. H. MacDonald, A. R. Mahon, L. A. Allers, J. F. Hassard, A. Mainwood, R. J. Ott. *Nucl. Instr. Methods Phys. Res. A* **1997**, *392*, 227.
[21] P. F. Morrissey, S. R. McCandliss, P. D. Feldman, S. D. Friedman. *Appl. Opt.* **1994**, *33*, 2534.
[22] K. R. McIntosh, G. Lau, J. N. Cotsell, K. Hanton, D. L. Bätzner, F. Bettiol, B. S. Richards. *Prog. Photovolt: Res. Appl.* **2009**, *17*, 191.
[23] J. Janesick, Scientific Charge Coupled Devices, SPIE, Bellingham, WA, USA, **2001**.
[24] (a) Cambridge Structural Database, F. H. Allen. *Acta Crystallogr. Sect. B*, **2002**, *58*, 380; (b) F. H. Allen, W. D. S. Motherwell, *Acta Crystallogr. Sect. B* **2002**, *58*, 407. (c) CSD version 5.32, updated Feb. 2011. http://www.ccdc.cam.ac.uk
[25] H. Görner, S. Khanra, T. Weyhermüller, P. Chaudhuri. *J. Phys. Chem. A* **2006**, *110*, 2587.
[26] W. Tang, Y. Xiang, A. Tong. *J. Org. Chem.* **2009**, *74*, 2163.
[27] X. Chen, R. Wei, X. Xiang, Z. Zhou, K. Li, P. Song, A. Tong. *J. Phys. Chem. C* **2011**, *115*, 14353.
[28] J. Grzegorzek, Z. Mielke, A. Filarowski. *J. Mol. Struct.* **2010**, *976*, 371.
[29] M. Oki, Applications of Dynamic NMR Spectroscopy to Organic Chemistry, VCH Publishers, Deerfield Beach, USA, **1985**, pp. 364–365.
[30] S.-I. Liu. *J. Comput. Chem.* **2009**, *30*, 2176.
[31] T. Hökelek, S. Bílge, Z. Kilic. *Anal. Sci.* **2006**, *22*, x115.
[32] S. Berger, S. Braun, 200 and More NMR Experiments, Wiley-VCH, Weinheim, **2004**.
[33] R. G. Parr, W. Yang, Density-Functional Theory of Atoms and Molecules, Oxford Science Publications: Oxford, New York, **1989**.
[34] L. J. Bartolotti, K. Fluchick Reviews in Computational Chemistry, vol. *7* (eds: K. B. Lipkowitz, D. B. Boyd), VCH Publishers, NewYork, **1996**; p. 187.
[35] M. J. Frisch, J. A. Pople, R. Krishnam, J. S. Binkley. *J. Chem. Phys.* **1984**, *80*, 3265.
[36] Gaussian 09, Revision A.1, M. J. Frisch, G. W. Trucks, H. B. Schlegel, G. E. Scuseria, M. A. Robb, J. R. Cheeseman, G. Scalmani, V. Barone, B. Mennucci, G. A. Petersson, H. Nakatsuji, M. Caricato, X. Li, H. P. Hratchian, A. F. Izmaylov, J. Bloino, G. Zheng, J. L. Sonnenberg, M. Hada, M. Ehara, K. Toyota, R. Fukuda, J. Hasegawa, M. Ishida, T. Nakajima, Y. Honda, O. Kitao, H. Nakai, T. Vreven, J. A. Montgomery, Jr., J. E. Peralta, F. Ogliaro, M. Bearpark, J. J. Heyd, E. Brothers, K. N. Kudin, V. N. Staroverov, R. Kobayashi, J. Normand, K. Raghavachari, A. Rendell, J. C. Burant, S. S. Iyengar, J. Tomasi, M. Cossi, N. Rega, J. M. Millam, M. Klene, J. E. Knox, J. B. Cross, V. Bakken, C. Adamo, J. Jaramillo, R. Gomperts, R. E. Stratmann, O. Yazyev, A. J. Austin, R. Cammi, C. Pomelli, J. W. Ochterski, R. L. Martin, K. Morokuma, V. G. Zakrzewski, G. A. Voth, P. Salvador, J. J. Dannenberg, S. Dapprich, A. D. Daniels, Ö. Farkas, J. B. Foresman, J. V. Ortiz, J. Cioslowski, and D. J. Fox, Gaussian, Inc., Wallingford CT, **2009**.

[37] J. W. McIver, A. K. Komornicki. *J. Am. Chem. Soc.* **1972**, *94*, 2625.
[38] R. Ditchfield. *Mol. Phys.* **1974**, *27*, 789.
[39] F. London. *J. Phys. Radium* **1937**, *8*, 397.
[40] J. Tomasi, B. Mennucci, R. Cammi. *Chem. Rev.* **2005**, *105*, 2999.
[41] F. Blanco, I. Alkorta, J. Elguero. *Magn. Reson. Chem.* **2007**, *45*, 797.
[42] J. Pinto, V. L. M. Silva, A. M. S. Silva, R. M. Claramunt, D. Sanz, M. C. Torralba, M. R. Torres, F. Reviriego, I. Alkorta, J. Elguero. *Magn. Reson. Chem.* **2013**, *51*, 203.
[43] P. Giannozzi, S. Baroni, N. Bonini, M. Calandra, R. Car, C. Cavazzoni, D. Ceresoli, G. L. Chiarotti, M. Cococcioni, I. Dabo, A. Dal Corso, S. Fabris, G. Fratesi, S. de Gironcoli, R. Gebauer, U. Gerstmann, C. Gougoussis, A. Kokalj, M. Lazzeri, L. Martin-Samos, N. Marzari, F. Mauri, R. Mazzarello, S. Paolini, A. Pasquarello, L. Paulatto, C. Sbraccia, S. Scandolo, G. Sclauzero, A. P. Seitsonen, A. Smogunov, P. Umari, R. M. Wentzcovitch, *J. Phys. Condens. Matter* **2009**, *21*, 395502-19, www-quantum-espresso.org
[44] S. Grimme. *J. Comput. Chem.* **2004**, *25*, 1463–1473.
[45] S. Grimme. *J. Comput. Chem.* **2006**, *27*, 1787–1799.
[46] S. Grimme, J. Antony, S. Ehrlich, H. Krieg. *J. Chem. Phys.* **2010**, *132*, 154104–154123.
[47] J. P. Perdew, K. Burke, M. Ernzerhof. *Phys. Rev. Lett.* **1996**, *77*, 3865–3868.
[48] J. P. Perdew, K. Burke, Y. Wang. *Phys. Rev. B* **1996**, *54*, 16533–16539.
[49] V. Bertolasi, P. Gilli, V. Ferretti, G. Gilli, K. Vaughan. *New J. Chem.* **1999**, *23*, 1261.
[50] A. C. Olivieri, R. B. Wilson, I. C. Paul, D. Y. Curtin. *J. Am. Chem. Soc.* **1989**, *111*, 5525.
[51] S. H. Alarcón, A. C. Olivieri, M. González-Sierra. *J. Chem. Soc. Perkin Trans.* **1994**, *2*, 1067.
[52] A. R. Katritzky, I. Ghiviriga, P. Leeming, F. Soti. *Magn. Reson. Chem.* **1996**, *34*, 518.
[53] M. Jaworska, P. B. Hrynczyszyn, M. Welniak, A. Wojtzcak, K. Nowicka, G. Krasinski, W. Ciesielski, M. J. Potrzebowski. *J. Phys. Chem. A* **2010**, *114*, 12522.
[54] Z. Rozwadowski, E. Majewski, T. Dziembowska, P. E. Hansen. *J. Chem. Soc. Perkin Trans.* **1999**, *2*, 2809.
[55] L. Racané, Z. Mihalic, H. Ceric, J. Popovic, V. Tralic-Kulenovic. *Dyes Pigm.* **2013**, *96*, 672.
[56] S. H. Alarcón, A. C. Olivieri, D. Sanz, R. M. Claramunt, J. Elguero. *J. Mol. Struct.* **2004**, *705*, 1.
[57] S. H. Alarcón, A. C. Olivieri, P. Jonsen. *J. Chem. Soc. Perkin Trans.* **1993**, *2*, 1783.
[58] H. Joshi, F. S. Kamounah, G. v. d. Zwan, C. Gooijer, L. Antonov. *J. Chem. Soc. Perkin Trans.* **2001**, *2*, 2303.
[59] W. M. F. Fabian, L. Antonov, D. Nedeltcheva, F. S. Kamounah, P. J. Taylor. *J. Phys. Chem. A* **2004**, *108*, 7603.
[60] S. Sharif, G. S. Denisov, M. D. Toney, H. H. Limbach. *J. Am. Chem. Soc.* **2006**, *128*, 3375.
[61] N. S. Golubev, S. N. Smirnov, P. M. Tolstoy, S. Sharif, M. D. Toney, G. S. Denisov, H. H. Limbach. *J. Mol. Struct.* **2007**, *844-845*, 319.
[62] J. Elguero, C. Marzin, A. R. Katritzky, P. Linda, The Tautomerism of Heterocycles, Academic Press, New York, **1976**, pp. 29.
[63] H. Y. Lee, X. Song, H. Park, M.-H. Baik, D. Lee. *J. Am. Chem. Soc.* **2010**, *132*, 12133.
[64] A. S. Özen, P. Doruker, V. Aviyente. *J. Phys. Chem. A* **2007**, *111*, 13506.
[65] A. Golcu, M. Tumer, H. Demirelli, R. A. Wheatley. *Inorg. Chim. Acta* **2005**, *358*, 1785.
[66] N. Galic, Z. Cimerman, V. Tomisic. *Spectrochim. Acta A* **2008**, *71*, 1274.
[67] D. Ruiz-Molina, J. Veciana, K. Wurst, D. N. Hendrickson, C. Rovira. *Inorg. Chem.* **2000**, *39*, 617.
[68] W. You, H.-Y. Zhu, W. Huang, B. Hu, Y. Fan, X.-Z. You. *Dalton Trans.* **2010**, *39*, 7876.
[69] P. Fita, E. Luzina, T. Dziembowska, D. Kopec, P. Piatkowski, C. Radzewicz, A. Grabowska. *Chem. Phys. Lett.* **2005**, *416*, 305.
[70] M. Ziólek, J. Kubicki, A. Maciejewski, P. Naskrecki, A. Grabowska. *J. Chem. Phys.* **2006**, *124*, 124518.